

Alma Mater Studiorum Università di Bologna
Archivio istituzionale della ricerca

IL-25 participates in keratinocyte-driven dermal matrix turnover and is reduced in systemic sclerosis epidermis

This is the final peer-reviewed author's accepted manuscript (postprint) of the following publication:

Published Version:

Russo, B., Borowczyk, J., Cacialli, P., Moguelet, P., Truchetet, M.-E., Modarressi, A., et al. (2022). IL-25 participates in keratinocyte-driven dermal matrix turnover and is reduced in systemic sclerosis epidermis. RHEUMATOLOGY, 61(11), 4558-4569 [10.1093/rheumatology/keac044].

Availability:

This version is available at: <https://hdl.handle.net/11585/908721> since: 2022-12-02

Published:

DOI: <http://doi.org/10.1093/rheumatology/keac044>

Terms of use:

Some rights reserved. The terms and conditions for the reuse of this version of the manuscript are specified in the publishing policy. For all terms of use and more information see the publisher's website.

This item was downloaded from IRIS Università di Bologna (<https://cris.unibo.it/>).
When citing, please refer to the published version.

(Article begins on next page)

This is the final peer-reviewed accepted manuscript of:

Russo B.; Borowczyk J.; Cacialli P.; Moguelet P.; Truchetet M.-E.; Modarressi A.; Brembilla N.C.; Bertrand J.; Boehncke W.-H.; Chizzolini C.: *IL-25 participates in keratinocyte-driven dermal matrix turnover and is reduced in systemic sclerosis epidermis*

RHEUMATOLOGY VOL. 61 ISSN 1462-0332

DOI: 10.1093/rheumatology/keac044

The final published version is available online at:

<https://dx.doi.org/10.1093/rheumatology/keac044>

Terms of use:

Some rights reserved. The terms and conditions for the reuse of this version of the manuscript are specified in the publishing policy. For all terms of use and more information see the publisher's website.

This item was downloaded from IRIS Università di Bologna (<https://cris.unibo.it/>)

When citing, please refer to the published version.

1
2
3
4
5
6
7
8
9
10
11
12
13
14
15
16
17
18
19
20
21
22
23
24
25
26
27
28
29
30
31
32
33
34
35
36
37
38
39
40
41
42
43
44
45
46
47
48
49
50
51
52
53
54
55
56
57
58
59
60

IL-25 participates in keratinocyte-driven dermal matrix turnover and is reduced in Systemic Sclerosis epidermis

Barbara Russo^{1,2}, Julia Borowczyk¹, Pietro Cacialli¹, Philippe Moguelet³, Marie-Elise Truchetet⁴, Ali Modarressi⁵, Nicolò C. Brembilla^{1,2}, Julien Bertrand¹, Wolf-Henning Boehncke^{1,2}, Carlo Chizzolini^{1,6}

Affiliations

- ¹ Pathology & Immunology, School of Medicine, University of Geneva, Switzerland
- ² Department of Dermatology, University Hospital and School of Medicine, University of Geneva, Switzerland.
- ³ Department of Pathology, Tenon Hospital APHP, Paris, France
- ⁴ Department of Rheumatology, University Hospital, Bordeaux, France.
- ⁵ Plastic, reconstructive & aesthetic unit, University Hospital and School of Medicine, Geneva, Switzerland
- ⁶ Immunology & Allergy, Department of internal medicine, University Hospital and School of Medicine, Geneva, Switzerland

Corresponding author

Carlo Chizzolini; Pathology and Immunology, University Medical Center, Geneva University, Rue Michel-Servet 1, 1206 Geneva, Switzerland
e-mail: carlo.chizzolini@unige.ch, ORCID: 0000-0003-4849-6335

Running head: IL-25 in skin fibrosis.

Russo B et al.

IL-25 in skin fibrosis

Abbreviations: BM: basement membrane; Col-I: type-I collagen; ECM: extracellular matrix; HD: healthy donor; HDF: healthy donor fibroblast; GO: gene ontology; IL: interleukin; ILC-2: innate lymphoid cells-2; IL-1RA: interleukin-1 receptor antagonist; IF: immunofluorescence; IH: in situ hybridization; IHC: immunohistochemistry; KCM: keratinocyte-conditioned medium; MFI: mean fluorescence intensity, MMP, matrix metalloproteinase; SSc, systemic sclerosis; TGF- β , transforming growth factor- β ; TNF, tumor necrosing factor; TSLP: thymic stroma lymphopoietin.

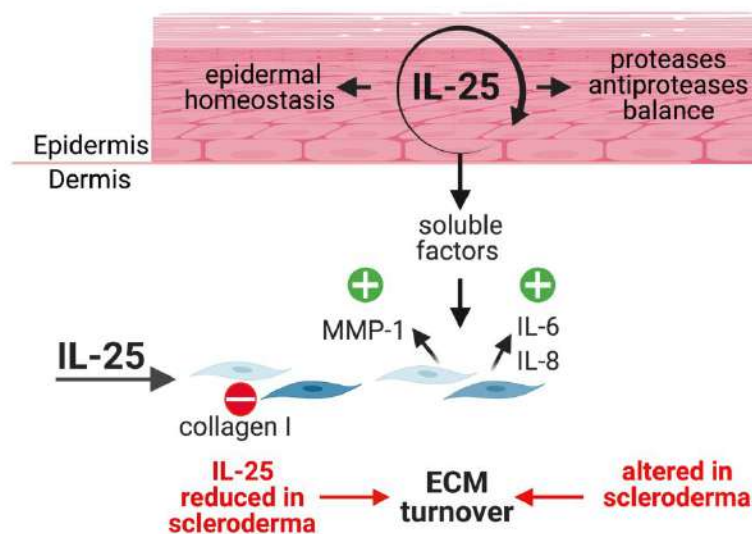
Russo B et al.

IL-25 in skin fibrosis

Keywords:

Scleroderma, Systemic Sclerosis, Skin, Fibrosis, IL-25, IL-17E, Epidermis, Keratinocytes, Extra cellular matrix, Fibroblast

Visual abstract



Key messages

- SSc epidermis is characterized by a reduced expression of IL-25
- The relative lack of IL-25 may alter dermal homeostasis favoring a reduced ECM reabsorption

1

2

3

4

5

6

7

8

9

10

11

12

13

14

15

16

17

18

19

20

21

22

23

24

25

26

27

28

29

30

31

32

33

34

35

36

37

38

39

40

41

42

43

44

45

46

47

48

49

50

51

52

53

54

55

56

57

58

59

60

Russo B et al.

IL-25 in skin fibrosis

- This perspective may contribute to better understanding of SSc and other fibrotic skin disorders

Introduction

Skin fibrosis, a hallmark of systemic sclerosis (SSc), is characterized by excessive deposition of extracellular matrix (ECM) in the dermis (1). The mechanisms involved in skin fibrosis remain poorly understood, but it is commonly accepted that inflammation due to vasculopathy and immune activation concurs to abnormal fibroblast activation leading to fibrogenesis (2). Recent evidence suggests that keratinocytes may also take part in skin fibrosis (3). Interestingly, SSc keratinocytes show a dysfunctional phenotype with aberrant differentiation and enhanced production/accumulation of inflammatory mediators (4-6). In SSc and keloids, dysfunctional keratinocytes may establish pathological interactions with fibroblasts skewing ECM turnover in favor of enhanced deposition, in addition to increased production of inflammatory mediators and growth factors by fibroblasts (6-8).

IL-25, also known as IL-17E, is a low-homology member of the IL-17 family, which uses the heterodimer IL-17RA / IL-17RB to signal (9, 10). Originally described as a Th2-type cytokine produced by hematopoietic cells (11), IL-25 is currently considered important in maintaining barrier integrity and homeostasis at mucosal and cutaneous surfaces when produced by epithelial cells. Further, IL-25 produced by keratinocytes appears to be a key inflammatory mediator in diseases as diverse as psoriasis (12-14), atopic dermatitis (15, 16), and contact dermatitis (17).

Little is known about the role of IL-25 in fibrosis and particularly in dermal fibrosis. In the lung, however, epithelial-derived IL-25 is thought to participate in fibrosis and airway remodeling both by its action on innate lymphoid cells 2 (ILC2) and macrophages and by modulating epithelial-mesenchymal transition in the context of allergic lung inflammation and in idiopathic lung fibrosis (18-20). Furthermore, IL-25 in conjunction with IL-33 and thymic stroma lymphopoietin (TSLP) was identified as a key mediator in various murine models of

organ fibrosis (21). Serum levels of IL-25 have been reported to be increased in SSc (22) and the number of IL-25 positive cells increased in SSc dermis (23), however no study addressed the potential role of IL-25 within SSc skin fibrosis. To this aim, we assessed the presence of IL-25 in SSc epidermis and the autocrine effect of IL-25 on keratinocytes as well as the effect of IL-25 on keratinocyte-driven fibroblast activation. Our results indicate that IL-25 is decreased in SSc epidermis. Further, under the influence of IL-25, healthy keratinocytes enhance inflammatory cytokines and matrix metalloproteinase-1 but not type I collagen production by fibroblasts, consequently acting as negative regulators of ECM deposition. Thus, IL-25 deficiency in SSc may contribute to dermal fibrosis.

Russo B et al.

IL-25 in skin fibrosis

Methods

Detailed materials and methods are provided as in Supplementary Data S1, available at *Rheumatology* online.

Human samples

All SSc patients fulfilled the 2013 ACR/EULAR classification criteria. Their clinical characteristics are reported in Supplementary Table S6, available at *Rheumatology* online. Punch biopsies were obtained from SSc affected skin. Surgical biopsies were obtained from age- and sex-matched HD undergoing aesthetic surgery (abdominoplasty) at the Department of Plastic, Reconstructive, and Aesthetic Surgery of Geneva University Hospital (Geneva, Switzerland). None of the healthy donors had dermatological disorders. This study was approved by the ethical committee (06-063, Commission cantonale d'éthique de la recherche, Geneva, Switzerland) and was conducted according to the Declaration of Helsinki. Written informed consent was obtained from each individual.

Cell cultures and epidermal equivalent (EE) engineering

Primary human dermal fibroblasts and keratinocytes were isolated from HD and SSc skin, as described (24). EE were generated according to (14). Briefly, 5×10^5 HD keratinocytes were plated onto ThinCert cell culture inserts (Greiner Bio-One GmbH, Kremsmünster, Austria) and grown to confluence in CnT-Prime medium (CELLnTEC AG, Bern, Switzerland). After three days, the medium was switched to the CnT-Prime 3D Barrier medium, and the cells cultured at the air-liquid interface for 11 days. Fresh medium containing or not IL-25 (100 ng/ml) was replaced every other day. On the last day of culture, conditioned medium was collected and immediately frozen. EE were harvested and used for mRNA isolation or histology.

RNA sequencing analysis

The library preparation, sequencing, and read mapping to the reference genome were performed by the Genomics Platform at the University of Geneva (Switzerland) as described in supplementary material and methods.

The differential expression analysis was performed using R/Bioconductor package edgeR v.3.18.1. Paired t-test was used to assess the differentially expressed genes (DEG) and p-values were corrected for multiple testing errors with 5% false discovery rate (FDR) according to Benjamini-Hochberg (BH).

The **D**atabase for **A**notation, **V**isualization and **I**ntegrated **D**iscovery (**DAVID**) v6.8 was used for functional analysis of DEG and Gene Ontology (GO) database queried for DEG with FDR < 0.05 and log fold change (logFC) ≤ 2 or ≥ 2 . The Functional Annotation Clustering method was used to perform cluster analysis, selecting high classification stringency. Pathway and network analysis was performed using MetaCore™ (Cortellis Solution software; Clarivate Analytics, London, United Kingdom) or g:GOST (g: profiler, by ELIXIR) with an FDR < 0.05. Row data are stored under GSE168312.

Statistical analysis

Statistical analysis was performed with GraphPad Prism, version 8 (Graphpad Software, La Jolla, CA). Shapiro-Wilk normality test was used to evaluate normal distribution. Accordingly, statistical significance was assessed by paired Student t-test; Wilcoxon test. The non-parametric, two samples, Kolmogorov Smirnov test was used to assess differences in IL-25 epidermal distribution between groups. P-values ≤ 0.05 were considered statistically significant.

Results

IL-25 expression is decreased in the epidermis of SSc and scleroderma-like disorders

In healthy skin, IL-25 mostly accumulates in the granular layer of the epidermis (12). We asked the question whether this was the case also in SSc involved skin. By immunofluorescence we found that IL-25 was enriched in the granular layer of SSc epidermis, but the intensity of the signal was much fainter in SSc than in healthy donors (HD) (Figure 1a). The fluorescence intensity of IL-25, as assessed by automated quantification, was significantly lower in 10 SSc than in 7 HD, specifically in the granular layer of the epidermis ($p < 0.0001$) (Figure 1b). Individuals with diffuse cutaneous (dc)SSc ($n=5$) and limited (lc)SSc ($n=5$) exhibited similar IL-25 decreased expression (not shown), indicating that IL-25 is reduced in involved SSc epidermis. To substantiate our findings, we assessed the presence of IL-25 mRNA within the skin of 3 SSc patients and 3 HD by chromogenic *in situ* hybridization. Keratinocytes were found positive for IL-25 mRNA and consistently with the immunofluorescence data SSc keratinocytes expressed lower levels of IL-25 mRNA compared to HD (Figure 1c). We then tested whether the common receptor IL17RA and the IL-25-specific receptor IL-17RB were expressed in skin keratinocytes. This was the case both in SSc and HD skin. Moreover, no differences were readily apparent in staining intensity of IL-17RB between SSc and HD skin (Supplementary Figure S1, available at *Rheumatology* online).

We then asked whether IL-25 was also dysregulated in the epidermis of other skin disorders characterized by dermal fibrosis including morphea ($n=6$) and eosinophilic fasciitis ($n=4$) in addition to SSc ($n=6$) and compared to HD ($n=10$). By immunohistochemistry we observed that IL-25 was mainly localized in the granular layer of the epidermis in all four conditions. However, the levels of IL-25 were lower in all analyzed diseases when compared to HD ($p <$

0.0001 for comparison with HD for each condition (Figure 1d, e). These results suggest that decreased IL-25 in the epidermis is a common feature of fibrotic skin conditions.

IL-25 regulates tissue remodeling related pathways in keratinocytes

To investigate the effects IL-25 on keratinocyte functions, we generated epidermal equivalents (EE) from 3 distinct HD primary keratinocytes (Supplementary Figure S2, available at *Rheumatology* online) and cultured them in the presence or not of IL-25 for 11 days.

Unsupervised analysis of expressed genes identified by RNAseq shows that IL-25 critically shape keratinocytes expression profiles (Supplementary Figure S3, available at *Rheumatology* online).

We, then identified 1491 differentially expressed genes (DEGs) in EE exposed to IL-25 compared to not exposed EE, 949 of which were downregulated and 542 were upregulated with a false discovery rate (FDR) ≤ 0.05 (Figure 2a; Supplementary Tables S1 and S2, available at *Rheumatology* online).

Functional annotation clustering of the gene ontology (GO) term enriched for the genes with a $\log_{2}FC \geq \pm 2$ revealed that IL-25 mainly regulated genes participating in epidermal homeostasis (cluster 1), proteolysis (cluster 2), products located in vesicles or extracellular compartments (cluster 3), chemotaxis (cluster 4), and cytokine responses (cluster 5) (Figure 2b). To further understand physiological or pathological processes enriched in IL-25 exposed EE we used Map Folders ontology from MetaCore database. Of note, tissue remodeling and wound healing were among the top 10 most significantly enriched processes ($p=8.533 \times 10^{-10}$; Supplementary Table S3, available at *Rheumatology* online) and the top five enriched pathways in this folder include ECM remodeling, cell matrix glycoconjugate, EGFR signaling,

and ERBB signaling (Figure 2c). Importantly, the detailed representation of the pathways most significantly enriched suggests that keratinocytes cultured in the presence of IL-25 may participate in enhanced ECM remodeling by regulating protease activations (Figure 2d). To substantiate some of these findings, we tested whether MMP9, upregulated at the mRNA level by IL-25, was also regulated at the protein level. Indeed, we found that MMP9 was upregulated at protein level (Fig 2E) thus mimicking the results observed by RNAseq (Fig 2A) and highlighted when IL-25 regulated pathways were analyzed by MetaCore (Fig 2D). Enrichment analysis of DEG in EE treated with IL-25 using more databases (KEGG, REACTOME, GO) also revealed that several ECM related pathways are regulated by IL-25 in keratinocytes (Supplementary Figure S3 and Supplementary Table S4, available at *Rheumatology* online). Altogether these data suggests that IL-25 is involved in modulation of keratinocyte-ECM crosstalk.

IL-25 priming of keratinocytes enhances paracrine fibroblast inflammatory responses

We and others have previously demonstrated that keratinocytes, by releasing soluble mediators, may affect the functional capabilities of dermal fibroblasts (6-8, 24). Thus, we investigated to which extent IL-25 modulates the interaction between keratinocyte and fibroblast. To this aim, we established several culture conditions (Figure 3a, Supplementary Figure S4, available at *Rheumatology* online) using HD or SSc keratinocytes primed or not with IL-25 for 24h to generate keratinocyte conditioned media (KCM). KCM were then added to HD dermal fibroblasts (HDF) and their production of inflammatory mediators (IL-6, IL-8), matrix metalloproteinase-1 (MMP1), and the matrix proteins type-I collagen (Col-I) and fibronectin was then assessed as read out. KCM were added at 12.5% on fibroblast cultures. We observed that at the dose contained in KCM, when applied directly on fibroblasts, IL-25 did not induce substantial responses (gray symbols in

Figure 3b, c, d, e). As expected, KCM strongly (by 10 to 1000 fold) enhanced the production of IL-6, IL-8, and MMP-1 (Figure 3b, c, d; Supplementary Table S5, available at *Rheumatology* online). However, no major effects were observed for Col-I (Figure 3e) and fibronectin (Supplementary Figure S5) production. The magnitude of these responses was in general similar when KCM were generated from HD (blue) or SSc (pink) keratinocytes, but the magnitude of IL-6 and MMP-1 production was greater in the presence of KCM generated from SSc keratinocytes. Interestingly, KCM generated from IL-25-primed keratinocytes (IL-25⁺KCM) induced - or tended to induce - stronger inflammatory responses by fibroblasts compared to IL-25 non-primed keratinocytes. The production of fibronectin and col-I was similar in HDF cultured with IL-25⁺ or IL-25⁻ KCM either from HD or SSc keratinocytes. However, KCM skewed the ratio of collagen-I to MMP1, which was in favor of collagen degradation, more so in the presence of IL-25⁺KCM (Figure 3f). Of note, none of the biomarkers we assessed reached the assay detection level in KCM, which indicates that fibroblasts were the only/predominant producing cells in our assays. Overall, these results indicate that IL-25-primed keratinocytes enhance the inflammatory IL-6, IL-8, and MMP-1 fibroblast responses. In addition, by favoring MMP-1 over Col-I production they may tip the balance in favor of ECM degradation rather than deposition. Given these findings, we assessed the effect of IL-25 to directly prime dermal fibroblasts. In these assays, where TGF- β as expected enhanced Col-I production, IL-25 at 100 ng/ml significantly reduced the Col-I production by 1.8-fold, $p=0.02$ in HD fibroblasts; a reduction similar to that reached by TNF (Figure 4). Findings at mRNA level are shown in Supplementary Figure S6. Intriguingly, SSc fibroblasts did not show a significant reduced production of collagen in response to both IL-25 and TNF. Whereas TNF powerfully enhanced MMP-1 production, IL-25 did not modify the levels of MMP-1 produced by fibroblasts. However, the overall result of the direct priming of dermal fibroblasts with IL-25 was a decreased Col-I to MMP-1 ratio (Figure 4). This was distinctly different from the pro-fibrotic

effect observed in the presence of TGF- β with enhanced Col-I to MMP-1 ratio and supports the contention that IL-25 by its direct effects on fibroblasts as well as by its indirect effects through keratinocytes tips the Col-I to MMP-1 balance favoring enhanced ECM degradation, thus exerting, at least *in vitro*, an anti-fibrotic effect.

In addition, we observed that IL-25 partially inhibited α -smooth muscle actin (α -SMA) expression promoted by TGF β in dermal fibroblasts (Supplementary Figure S7, available at *Rheumatology* online), further suggesting that IL-25 may preferentially restrain fibrosis.

Early keratinocyte responses to IL-25 suggest the release of preformed mediators.

To communicate with neighboring cells, including dermal fibroblasts, keratinocytes may release preformed and stored material (25). We conducted time-dependent experiments to test the hypothesis that IL-25 could enhance this phenomenon. We observed that the production of IL-6 by dermal fibroblasts was significantly enhanced when fibroblasts were exposed to conditioned medium generated from keratinocytes primed by IL-25 (IL-25+KCM) for 10 min only. Similar results were obtained when keratinocytes were primed with IL-25 for 30 min (Figure 5a). The enhancing effect over control keratinocyte conditioned medium (KCM) was present also when keratinocytes were primed with IL-25 for 4h and 24 h. However, the effect over background of non-primed KCM became evident at these later time points (Figure 5a). The enhancing effect of 10 min IL-25+KCM was not due to IL-25 carryover since the neutralization of IL-25 in IL-25+KCM added to fibroblasts did not modify the results (Figure 5b). Furthermore, the effect of 10 min priming of keratinocytes with IL-25 was specific, since we did not observe such an effect when keratinocytes were primed with TNF (Figure 5c). This is relevant, since the conditioned medium of keratinocytes primed with TNF for 24 h induced a robust IL-6 production by fibroblasts (Figure 5c). Thus, the differential effects of short (10

min) versus long (24h) priming distinguish the activities of IL-25 and TNF on keratinocytes. Of interest, IL-17A shared with IL-25 the capacity to prime keratinocytes in 10 min time, resulting in higher IL-6 production by fibroblasts (Figure 5d). We then wondered whether the effects of IL-25 and IL-17A on keratinocytes were mediated by receptor binding. We observed that blockade of IL-17RA on keratinocytes resulted in the abrogation of the enhancing effect due to priming with IL-25 and IL-17A (Figure 5d). Finally, guided by the results obtained in similar settings (5, 6, 24), we tested whether IL-1 could be mediating the early as well as late effects of KCM. This was indeed the case since IL-1ra abrogated the IL-6 production by fibroblasts in response to IL-25+KCM obtained after 10 min and 24h (Figure 5e, f). Overall, these results suggest that IL-25 induces early keratinocyte responses (within 10 min) capable of activating fibroblasts, a characteristic shared with IL-17A.

Discussion

When initiating this work, we were hypothesizing that epidermal IL-25 would be increased in SSc. Against our hypothesis we found that SSc keratinocytes *ex vivo* express significantly lower amounts of IL-25 than healthy keratinocytes, a characteristic shared by other fibrotic skin disorders including morphea and eosinophilic fasciitis. Several were the supportive elements for our original hypothesis. First, serum IL-25 was reported to be increased in SSc (22), and IL-25 positive cells increased in SSc dermis (23). Second, IL-25, in conjunction with IL-33 and TSLP, was associated with fibrosis in several mouse models of fibrosis, particularly mediated by Th2 responses (21). Indeed, a predominant Th2-like environment characterizes SSc in which T cells producing IL-4 and/or IL-13, ILC2, as well as IL-33 and TSLP positive cells have been documented in SSc skin (26-31). Third, enhanced IL-25 expression by epithelial airway and alveolar cells was linked to lung fibrosis within asthma and idiopathic pulmonary fibrosis (18-20). *Vice versa*, for the first time, our work documents that a relative lack of IL-25 rather than its excess characterizes SSc epidermis and is distinctly different from psoriasis, atopic dermatitis, and contact dermatitis in which IL-25 epidermal expression is increased (12, 13, 15-17). Such an observation supports the hypothesis that an IL-25 epidermal deficiency could be implicated in skin fibrosis. However, we did not investigate the mechanism underlying the IL-25 dysregulation in SSc epidermis and further research is needed to address this finding.

The constitutive expression of IL-25 in healthy keratinocytes substantiate its role in skin homeostasis and is consistent with previous findings (32, 33). The information we obtained by assessing the effect of IL-25 on gene transcription in epidermal equivalents generated from healthy keratinocytes shows that IL-25 may regulate a wide variety of gene products located in vesicles or extracellular compartment and participating in epidermal homeostasis, proteolysis, chemotaxis, and IL-1 or TNF family members signaling. An important finding was

that IL-25 regulates molecular pathways involved in ECM turnover and remodeling by coordinating the expression of several proteases and antiproteases (such as MMP-9, MMP-7; MMP-12, TIMP3, SERPIN12, SERPIN1) (Fig 2a, d). This is intriguing because it is increasingly clear that the ECM architecture affects the availability of growth factors and cytokines and determine tissue stiffness, and that an altered ECM remodeling participate to fibrosis (34, 35). Furthermore, proteases may participate in vascular damage, crucial in SSc pathogenesis. For example, MMP-12 and MMP-7, both downregulated by IL-25, are increased in SSc skin and lung and their levels correlate with fibrosis severity and vascular damage (36). Consistently, there is evidence that MMP-12 deficiency attenuate skin fibrosis and angiotensin-II mediated vascular injury (37). Transcriptomic analysis also revealed that IL-25 negatively regulate a number of serin proteases, involved in fibrinolysis (such as SERPIN 12, SERPIN1). This is captivating because fibrinolysis is increased in SSc and is associated to vascular dysfunction and fibrosis in SSc (38). To complement RNAseq data, we also found that MMP9 protein levels were increased in EE by IL-25. Thus, a relative lack of IL-25 in SSc skin may result in less MMP9 available, which is consistent with the reported reduced MMP9 activity detected in SSc sera (39). Furthermore, we showed that, through its action on keratinocytes, IL-25 indirectly increases MMP-1 secretion by fibroblasts while it directly decreases their col-I production, supporting the hypothesis that IL-25 may favor ECM resorption over deposition in the skin. In this context, IL-25 deficiency in SSc epidermis may alter the protease-antiprotease balance and ECM composition, favoring the activation of some pathway crucial in SSc pathogenesis. Similarly, to our results, previous studies on lung fibrosis showed that IL-25 promoted protease activity, ECM remodeling, inflammatory responses, and regulated epithelial-mesenchymal cross-talk (18-20).

Russo B et al.

IL-25 in skin fibrosis

Of interest, our data suggest that IL-25-priming of keratinocytes could be, at least in part, associated with a receptor-mediated, enhanced secretion of pre-stored mediators, as supported by the observation that keratinocytes conditioned media collected after only 10 min was sufficient to promote a significant production of IL-6 by fibroblasts. We have not investigated the mechanisms underlying such an effect, but it appeared to be specific to IL-17 family members since TNF did not induce early keratinocyte responses while both IL-17A and IL-25 did and an anti-IL-17AR mAb blocked their effect. The capacity of keratinocytes to release prestored mediators, eventually in extracellular vesicles (EV) of various size, has been reported in the literature (25). Cellular stress induced by hypoxia, serum starvation, UV exposure, as well as keratinocyte stimulation by TGF- α , and poly I:C were described as factors favoring EV release (reviewed in (25)).

This paper has some limitations. To assess the differential expression of IL-25 between healthy and fibrotic skin we used immunohistology, that may be limited by semiquantitative quantification. However, the use of software-based signal quantification and the use of different techniques to assess the presence of IL-25 in keratinocytes permitted to minimize this point. We did not investigate why IL-25 is reduced in SSc patients. RNAseq analysis results were not validated at the protein level, and we did not successfully knock out the IL-25 gene in primary human keratinocyte to assess their function in the absence of the cytokine. However, we engineered epidermal equivalents allowing both keratinocyte proliferation and differentiation to study the effects of IL-25 on keratinocytes and focused on the role of IL-25 to modulate keratinocyte-generated mediators influencing fibroblast responses. By using larger numbers of keratinocytes - and biopsies - obtained from both limited and diffuse, as well as early vs late disease would increase the breath of our findings, possibly identifying

subset-related functions of IL-25. Further, the effect of IL-25-primed KCM on fibroblasts was assessed after 48 h of culture. This may hinder the possible secondary activities of cytokines induced by KCM, such as IL-6, which may secondarily result in enhanced collagen production. However, in other experimental systems in which IL-17 was added to organotypic skin cultures for 9 days, no such secondary effects were seen (24).

In conclusion, reduced expression of IL-25 characterizes SSc epidermis, and the relative lack of IL-25 may alter dermal homeostasis favoring deposition rather than ECM resorption. This perspective may contribute to better understanding SSc and other fibrotic skin disorders.

Acknowledgements: We thank Natacha Civic and Mylène Docquier (Genomics Platform) for performing the RNA sequencing; Nicolas Laudet (Bioimaging Core Facility) for quantification of immune-histology, François Prodon and Olivier Brun for microscope imaging (Bioimaging Core Facility), Marie Ebrahim Malek and Laura de Luca (Histology Core Facility) for contribution to tissue preparation (all at University Medical Center, Geneva, Switzerland).

Grants and financial support of the study: This work was supported in part by grant 310030-159999 from the Swiss National Science Foundation (SNSF) to CC, by a grant from the Swiss Scleroderma Patient organization (sclerodermie.ch) to CC; by grant 310030_152680 and 310030_175470/1 from SNSF to WHB, by grant 310030_184814 from SNSF to JB; by grant from the Ernst & Lucie Schmidheiny foundation to BR.

Conflicts of Interest

MET received honoraria as an advisor or invited speaker from Abbvie, Lilly, SOBI and Boehringer Ingelheim

Russo B et al.

IL-25 in skin fibrosis

WHB received honoraria as an advisor or invited speaker from Abbvie, Almirall, BMS, Celgene, Leo, Lilly, Novartis, and UCB

CC received honoraria as an advisor or invited speaker from GSK, Roche, Boehringer Ingelheim

The other authors have disclosed no conflicts of interest.

Data availability statement: Data will be available upon reasonable request to the corresponding author.

References

1. Allanore Y, Simms R, Distler O, Trojanowska M, Pope J, Denton CP, et al. Systemic sclerosis. *Nature reviews Disease primers*. 2015;1:15002.
2. Stern EP, Denton CP. The Pathogenesis of Systemic Sclerosis. *Rheum Dis Clin North Am*. 2015;41(3):367-82.
3. Russo B, Brembilla NC, Chizzolini C. Interplay Between Keratinocytes and Fibroblasts: A Systematic Review Providing a New Angle for Understanding Skin Fibrotic Disorders. *Frontiers in immunology*. 2020;11:648.
4. Aden N, Shiwen X, Aden D, Black C, Nuttall A, Denton CP, et al. Proteomic analysis of scleroderma lesional skin reveals activated wound healing phenotype of epidermal cell layer. *Rheumatology (Oxford)*. 2008;47(12):1754-60.
5. Aden N, Nuttall A, Shiwen X, de Winter P, Leask A, Black CM, et al. Epithelial cells promote fibroblast activation via IL-1alpha in systemic sclerosis. *J Invest Dermatol*. 2010;130(9):2191-200.

6. Russo B, Borowczyk J, Boehncke WH, Truchetet ME, Modarressi A, Brembilla NC, et al. Dysfunctional keratinocytes increase dermal inflammation in systemic sclerosis. Results from tissue-engineered scleroderma epidermis. *Arthritis & rheumatology*. 2021.

7. Nikitorowicz-Buniak J, Shiwen X, Denton CP, Abraham D, Stratton R. Abnormally differentiating keratinocytes in the epidermis of systemic sclerosis patients show enhanced secretion of CCN2 and S100A9. *J Invest Dermatol*. 2014;134(11):2693-702.

8. McCoy SS, Reed TJ, Berthier CC, Tsou PS, Liu J, Gudjonsson JE, et al. Scleroderma keratinocytes promote fibroblast activation independent of transforming growth factor beta. *Rheumatology (Oxford)*. 2017;56(11):1970-81.

9. McGeachy MJ, Cua DJ, Gaffen SL. The IL-17 Family of Cytokines in Health and Disease. *Immunity*. 2019;50(4):892-906.

10. Borowczyk J, Shutova M, Brembilla NC, Boehncke WH. IL-25 (IL-17E) in epithelial immunology and pathophysiology. *J Allergy Clin Immunol*. 2021.

11. Fort MM, Cheung J, Yen D, Li J, Zurawski SM, Lo S, et al. IL-25 induces IL-4, IL-5, and IL-13 and Th2-associated pathologies in vivo. *Immunity*. 2001;15(6):985-95.

12. Senra L, Stalder R, Alvarez Martinez D, Chizzolini C, Boehncke WH, Brembilla NC. Keratinocyte-Derived IL-17E Contributes to Inflammation in Psoriasis. *The Journal of investigative dermatology*. 2016;136(10):1970-80.

13. Xu M, Lu H, Lee YH, Wu Y, Liu K, Shi Y, et al. An Interleukin-25-Mediated Autoregulatory Circuit in Keratinocytes Plays a Pivotal Role in Psoriatic Skin Inflammation. *Immunity*. 2018;48(4):787-98.e4.

14. Borowczyk J, Buerger C, Tadjrischi N, Drukala J, Wolnicki M, Wnuk D, et al. IL-17E (IL-25) and IL-17A Differentially Affect the Functions of Human Keratinocytes. *The Journal of investigative dermatology*. 2020;140(7):1379-89.e2.

Russo B et al.

IL-25 in skin fibrosis

15. Aktar MK, Kido-Nakahara M, Furue M, Nakahara T. Mutual upregulation of endothelin-1 and IL-25 in atopic dermatitis. *Allergy*. 2015;70(7):846-54.
16. Leyva-Castillo JM, Galand C, Mashiko S, Bissonnette R, McGurk A, Ziegler SF, et al. ILC2 activation by keratinocyte-derived IL-25 drives IL-13 production at sites of allergic skin inflammation. *The Journal of allergy and clinical immunology*. 2020;145(6):1606-14.e4.
17. Suto H, Nambu A, Morita H, Yamaguchi S, Numata T, Yoshizaki T, et al. IL-25 enhances T(H)17 cell-mediated contact dermatitis by promoting IL-1 β production by dermal dendritic cells. *The Journal of allergy and clinical immunology*. 2018;142(5):1500-9.e10.
18. Hams E, Armstrong ME, Barlow JL, Saunders SP, Schwartz C, Cooke G, et al. IL-25 and type 2 innate lymphoid cells induce pulmonary fibrosis. *Proceedings of the National Academy of Sciences of the United States of America*. 2014;111(1):367-72.
19. Gouda MM, Bhandary YP. Acute Lung Injury: IL-17A-Mediated Inflammatory Pathway and Its Regulation by Curcumin. *Inflammation*. 2019;42(4):1160-9.
20. Xu X, Luo S, Li B, Dai H, Zhang J. Feature Article: IL-25 contributes to lung fibrosis by directly acting on alveolar epithelial cells and fibroblasts. *Exp Biol Med (Maywood)*. 2019;244(9):770-80.
21. Vannella KM, Ramalingam TR, Borthwick LA, Barron L, Hart KM, Thompson RW, et al. Combinatorial targeting of TSLP, IL-25, and IL-33 in type 2 cytokine-driven inflammation and fibrosis. *Science translational medicine*. 2016;8(337):337ra65.
22. Robak E, Gerlicz-Kowalczyk Z, Dzionkowska-Bartkowiak B, Wozniacka A, Bogaczewicz J. Serum concentrations of IL-17A, IL-17B, IL-17E and IL-17F in patients with systemic sclerosis. *Archives of medical science : AMS*. 2019;15(3):706-12.

23. Lonati PA, Brembilla NC, Montanari E, Fontao L, Gabrielli A, Vettori S, et al. High IL-17E and Low IL-17C Dermal Expression Identifies a Fibrosis-Specific Motif Common to Morphea and Systemic Sclerosis. *PLoS ONE*. 2014;9(8):e105008.

24. Dufour AM, Borowczyk-Michalowska J, Alvarez M, Truchetet ME, Modarressi A, Brembilla NC, et al. IL-17A dissociates inflammation from fibrogenesis in systemic sclerosis (scleroderma). *J Invest Dermatol*. 2020;140(1):103-12.

25. Than UTT, Leavesley DI, Parker TJ. Characteristics and roles of extracellular vesicles released by epidermal keratinocytes. *J Eur Acad Dermatol Venereol*. 2019;33(12):2264-72.

26. Parel Y, Akesson A, De Luca C, Dayer JM, Chizzolini C. CD4+CD8+ double positive (DP) T cells are characteristic of early fibrotic skin lesions in systemic sclerosis (SSc) (Abstract). *Swiss Med Wkly*. 2002;132:s35.

27. Fuschiotti P, Larregina AT, Ho J, Feghali-Bostwick C, Medsger TA, Jr. Interleukin-13-producing CD8+ T cells mediate dermal fibrosis in patients with systemic sclerosis. *Arthritis Rheum*. 2013;65(1):236-46.

28. Yanaba K, Yoshizaki A, Asano Y, Kadono T, Sato S. Serum IL-33 levels are raised in patients with systemic sclerosis: association with extent of skin sclerosis and severity of pulmonary fibrosis. *Clin Rheumatol*. 2011;30(6):825-30.

29. Vettori S, Cuomo G, Iudici M, D'Abrosca V, Giacco V, Barra G, et al. Early systemic sclerosis: serum profiling of factors involved in endothelial, T-cell, and fibroblast interplay is marked by elevated interleukin-33 levels. *J Clin Immunol*. 2014;34(6):663-8.

30. Christmann RB, Mathes A, Affandi AJ, Padilla C, Nazari B, Bujor AM, et al. Thymic Stromal Lymphopoietin Is Up-Regulated in the Skin of Patients With Systemic Sclerosis and Induces Profibrotic Genes and Intracellular Signaling That Overlap With Those Induced by Interleukin-13 and Transforming Growth Factor beta. *Arthritis Rheum*. 2013;65(5):1335-46.

Russo B et al.

IL-25 in skin fibrosis

31. Wohlfahrt T, Usherenko S, Englbrecht M, Dees C, Weber S, Beyer C, et al. Type 2 innate lymphoid cell counts are increased in patients with systemic sclerosis and correlate with the extent of fibrosis. *Ann Rheum Dis*. 2015.
32. Wang YH, Angkasekwinai P, Lu N, Voo KS, Arima K, Hanabuchi S, et al. IL-25 augments type 2 immune responses by enhancing the expansion and functions of TSLP-DC-activated Th2 memory cells. *J Exp Med*. 2007;204(8):1837-47.
33. Corrigan CJ, Wang W, Meng Q, Fang C, Eid G, Caballero MR, et al. Allergen-induced expression of IL-25 and IL-25 receptor in atopic asthmatic airways and late-phase cutaneous responses. *J Allergy Clin Immunol*. 2011;128(1):116-24.
34. Menou A, Duitman J, Crestani B. The impaired proteases and anti-proteases balance in Idiopathic Pulmonary Fibrosis. *Matrix Biol*. 2018;68-69:382-403.
35. Kryczka J, Boncela J. Proteases Revisited: Roles and Therapeutic Implications in Fibrosis. *Mediators Inflamm*. 2017;2017:2570154.
36. Manetti M, Guiducci S, Romano E, Bellando-Randone S, Conforti ML, Ibba-Manneschi L, et al. Increased serum levels and tissue expression of matrix metalloproteinase-12 in patients with systemic sclerosis: correlation with severity of skin and pulmonary fibrosis and vascular damage. *Ann Rheum Dis*. 2012;71(6):1064-72.
37. Stawski L, Haines P, Fine A, Rudnicka L, Trojanowska M. MMP-12 deficiency attenuates angiotensin II-induced vascular injury, M2 macrophage accumulation, and skin and heart fibrosis. *PloS one*. 2014;9(10):e109763.
38. Kanno Y. The Role of Fibrinolytic Regulators in Vascular Dysfunction of Systemic Sclerosis. *Int J Mol Sci*. 2019;20(3).
39. Kikuchi K, Kubo M, Hoashi T, Tamaki K. Decreased MMP-9 activity in the serum of patients with diffuse cutaneous systemic sclerosis. *Clin Exp Dermatol*. 2002;27(4):301-5.

Figure legends

Figure 1

IL-25 expression is decreased in the epidermis of SSc and scleroderma-like disorders.

Representative detection of IL-25 by **a)** immunofluorescence and **d)** immunohistochemistry. Dotted line depicts basement membrane (BM). **b)** IL-25 mean fluorescence intensity (MFI) as function of distance from BM. Symbols represent the mean MFI±SEM of 10SSc and 7HD. **c)** IL-25 mRNA (blue) *in situ* hybridization. **e)** IL-25 optical density (OD) as function of distance from BM. Symbols represent the mean OD±SEM of 10 HD (blue), 6 SSc (fuchsia), 4 eosinophilic fasciitis (brown), 6 morphea (light-blue). Nuclear counterstaining by **a)** DAPI **c)** Fast red, **d)** Hematoxylin. **b); e)** $p < 0.0001$ between each pathology and HD, significant difference assessed by Kolmogorov Smirnov test.

Figure 2

IL-25 regulates genes involved in epidermal homeostasis and ECM remodeling.

Gene expression in EE treated or not with IL-25 analyzed by RNAseq. **a)** DEG in IL-25 compared to control EE. **b)** Functional annotation clustering of GO terms for genes with a $\log_{2}FC \geq 2$ or ≤ -2 and an $FDR \leq 0.01$ (gene counts >3 and EASE Score <0.01), computed by DAVID. **c)** Top 5 pathways from the significantly enriched ($p < 0.00001$) folder: “tissue remodeling and wound healing” from MetaCore database. **d)** Representation of “ECM remodeling” map in MetaCore. Thermometers: gene up- (red) and down-regulated (blue) in EE-treated with IL-25. Squares represent relevant up- (red) or down (blue) regulated genes. Detailed legend is in Supplementary Data S2, available at *Rheumatology* online. **e)** Protein levels of MMP9 were quantified by Western blotting in EE reconstitute from 3 independent healthy donors

Russo B et al.

IL-25 in skin fibrosis

keratinocytes cultured 11 days in presence or not of IL-25. In Western blotting quantification (f), the numbers indicate the densitometric quantifications of MMP9 bands normalized to the corresponding α -tubulin band. Each dot represents an independent EE.

EE: epidermal equivalents

Figure 3

IL-25 keratinocyte priming enhances paracrine fibroblast inflammatory responses

a) Experimental design. HD fibroblasts (HDF) were cultured in the presence of 12.5% conditioned media (CM) from HD (blue) or SSc (pink) keratinocytes primed or not with IL-25 (IL-25⁺KCM). Keratinocyte culture medium \pm IL-25, with no cells, was used as negative control, HDF cultured with IL-25 (12.5 ng/mL) as control for possible carryover. IL-6, IL-8, MMP-1, and collagen-I levels assessed by ELISA in HDF supernatants. Circles represent KCM from independent donors. Horizontal lines represent medians. Wilcoxon signed-rank-test * \leq 0.05. KCM= CM from keratinocytes, IL-25⁺KCM= CM from keratinocytes primed with IL-25. Full data set reported in Supplementary Tables S3A and B, available at *Rheumatology* online.

Figure 4

IL-25 reduces type-I collagen production by HD fibroblasts

HD (blue dots) or SSc (pink dots) fibroblasts were cultured in the presence of IL-25 (100 ng/mL), TGF- β (10 ng/mL), TNF (1 ng/ml), or control medium (Ctrl). MMP-1 and col-I levels assessed by ELISA in fibroblast supernatants.

Results are expressed as fold-change from spontaneous production (Ctrl). Each dot represents a distinct donor. Horizontal continue lines depict the mean. Red dotted line depict control. Statistical differences were assessed by paired t-test. * \leq 0.05.

Figure 5

IL-25 promotes the release of fibroblast-activating factors by keratinocytes at early time points.

a) IL-6 production by HDF cultured with 12.5% control keratinocytes conditioned medium (KCM) or IL-25+KCM harvested at the indicated time points. **b, d)** anti-IL-25 polyclonal-Ab, anti-IL-17RA mAb, and irrelevant Ab (IgG) added to KCM (b) or keratinocytes (d) prior to HDF stimulation. **c)** HDF cultured with KCM, IL-25+KCM, IL-17A (IL-17A+KCM), or TNF (TNF+KCM) harvested after 10 min. **e, f)** IL-1ra (100 ng/ml) added to HDF before priming with KCM or IL-25+KCM collected at 10 min (**e**) or 24h (**f**). Results are expressed as fold-change from spontaneous production (Ctrl). For all panels $n \geq 3$; bars represent the mean \pm SEM. Wilcoxon signed-rank test was used to assess statistical significance. * $p \leq 0.05$; ** $p \leq 0.01$.

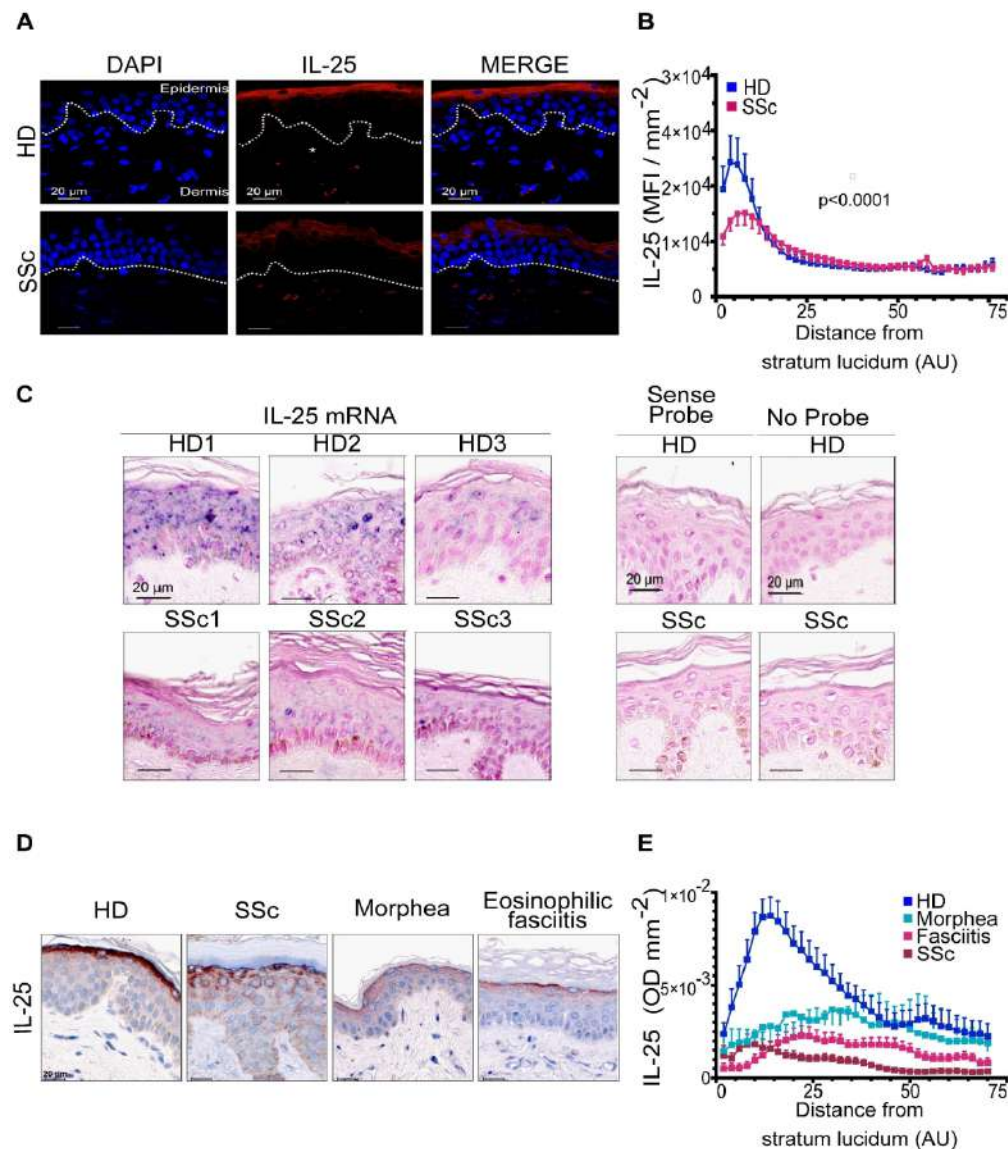


Figure 1

IL-25 expression is decreased in the epidermis of SSc and scleroderma-like disorders.

Representative detection of IL-25 by a) immunofluorescence d) immunohistochemistry.

Dotted line depicts basement membrane (BM). b) IL-25 mean fluorescence intensity (MFI) as function of distance from BM. Symbols represent the mean MFI \pm SEM of 10SSc and 7HD. c) IL-25 mRNA (blue) in situ hybridization. e) IL-25 optical density (OD) as function of distance from BM. Symbols represent the mean OD \pm SEM of 10 HD (blue), 6 SSc (fuchsia), 4 eosinophilic fasciitis (brown), 6 morphea (light-blue). Nuclear counterstaining by a) DAPI c) Fast red, d) Hematoxylin. b); e) $p < 0.0001$ between each pathology and HD, significant difference assessed by Kolmogorov Smirnov test.

186x212mm (300 x 300 DPI)

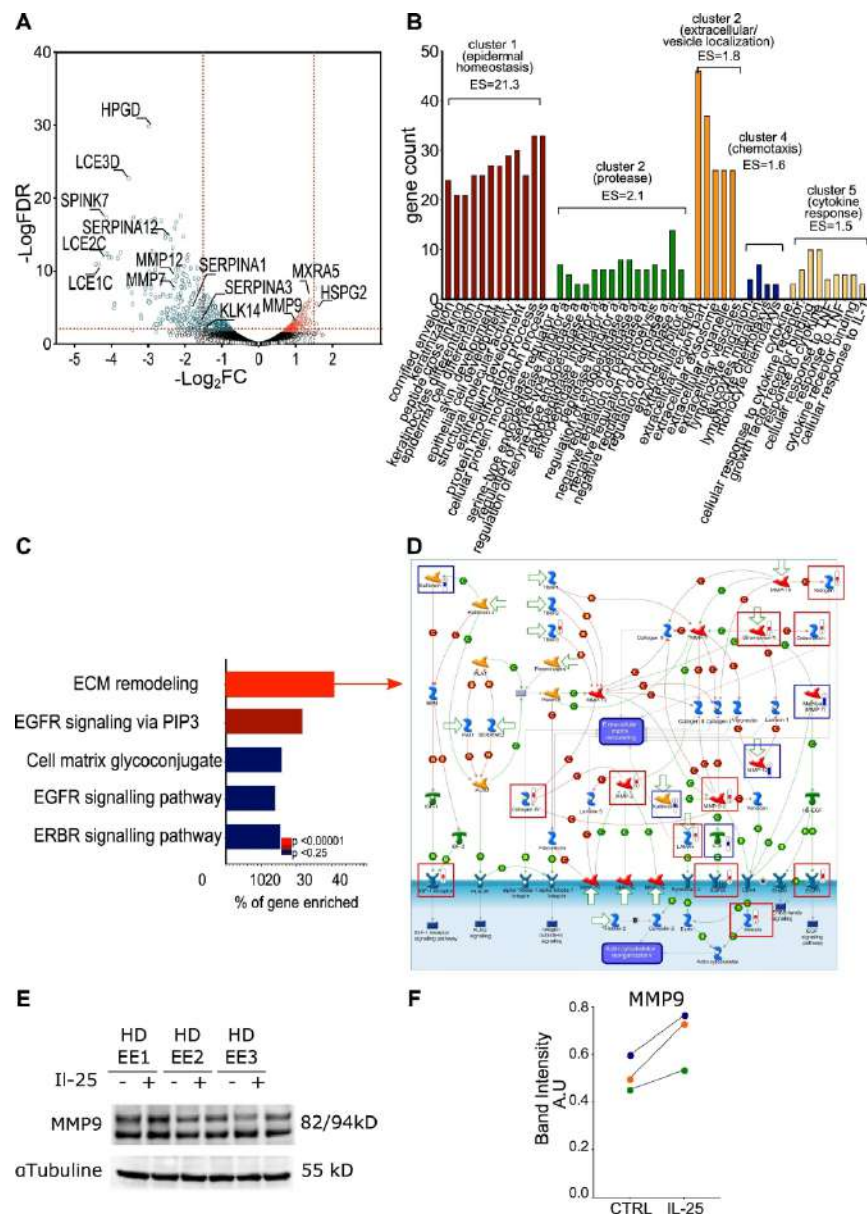


Figure 2
IL-25 regulates genes involved in epidermal homeostasis and ECM remodeling.
Gene expression in EE treated or not with IL-25 analyzed by RNAseq. a) DEG in IL-25 compared to control EE. b) Functional annotation clustering of GO terms for genes with a log₂FC ≥ 2 or ≤ -2 and an FDR ≤ 0.01 (gene counts >3 and EASE Score <0.01), computed by DAVID. c) Top 5 pathways from the significantly enriched (p < 0.00001) folder: "tissue remodeling and wound healing" from MetaCore database. d) Representation of "ECM remodeling" map in MetaCore. Thermometers: gene up- (red) and down-regulated (blue) in EE-treated with IL-25. Squares represent relevant up- (red) or down (blue) regulated genes. Detailed legend is in Supplementary legend to Figure 2. e) Protein levels of MMP9 were quantified by Western blotting in EE reconstitute from 3 independent healthy donors keratinocytes cultured 11 days in presence or not of IL-25. In Western blotting quantification (f), the numbers indicate the densitometric quantifications of MMP9 bands normalized to the corresponding α-tubulin band. Each dots represent an independent EE.

186x261mm (300 x 300 DPI)

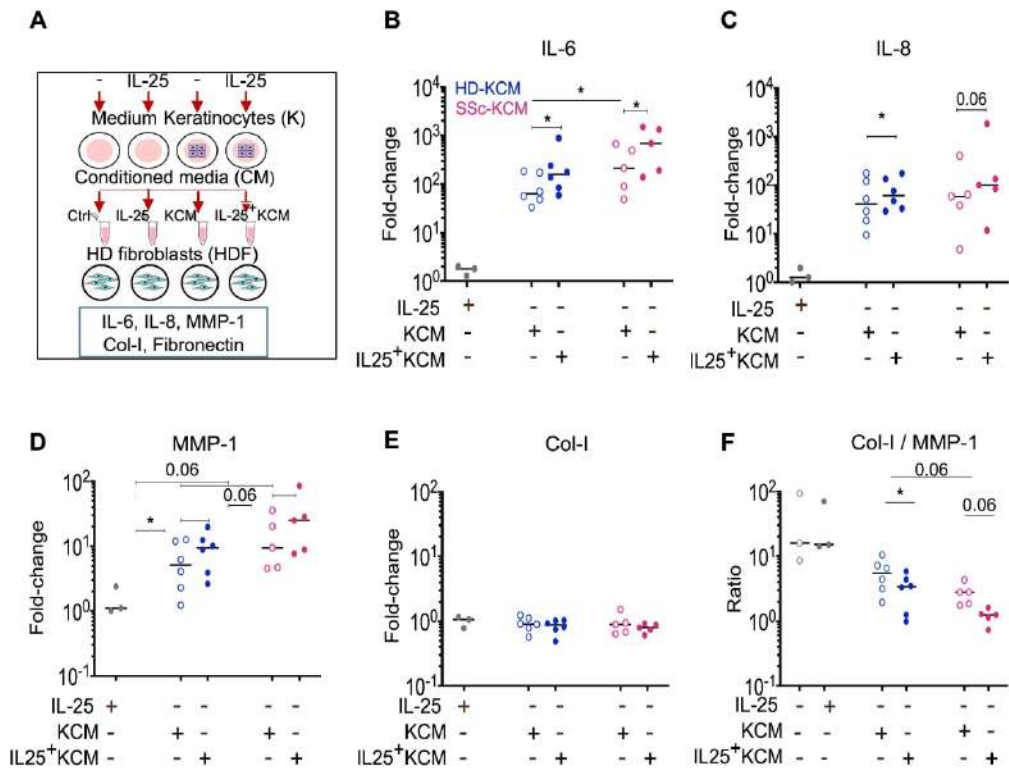


Figure 3

IL-25 keratinocyte priming enhances paracrine fibroblast inflammatory responses

a) Experimental design. HD fibroblasts (HDF) were cultured in the presence of 12.5% conditioned media (CM) from HD (blue) or SSc (pink) keratinocytes primed or not with IL-25 (IL-25+KCM). Keratinocyte culture medium \pm IL-25, with no cells, was used as negative control, HDF cultured with IL-25 (12.5 ng/mL) as control for possible carryover. IL-6, IL-8, MMP-1, and collagen-I levels assessed by ELISA in HDF supernatants. Circles represent KCM from independent donors. Horizontal lines represent medians. Wilcoxon signed-rank-test * ≤ 0.05 . KCM= CM from keratinocytes, IL-25+KCM= CM from keratinocytes primed with IL-25. Full data set reported in supplementary Tables S3A, B.

203x154mm (300 x 300 DPI)

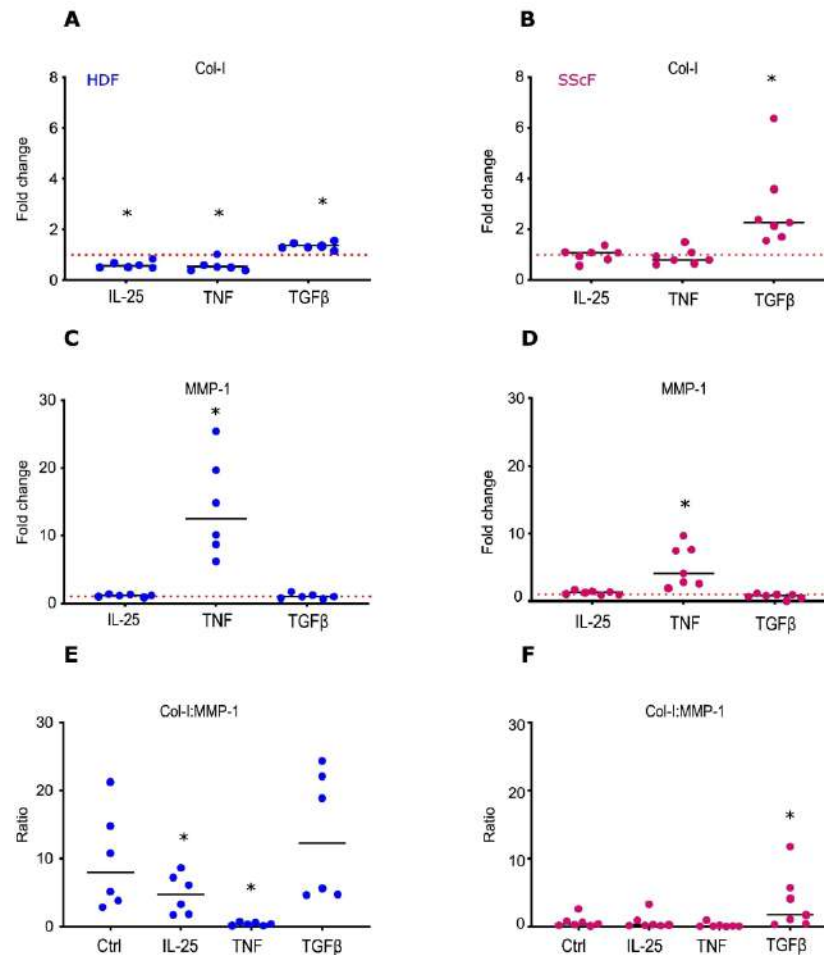


Figure 4

IL-25 reduces type-I collagen production by HD fibroblasts

HD (blue dots) or SSc (pink dots) fibroblasts were cultured in the presence of IL-25 (100 ng/mL), TGF- β (10 ng/mL), TNF (1 ng/mL), or control medium (Ctrl). MMP-1 and col-I levels assessed by ELISA in fibroblast supernatants.

Results are expressed as fold-change from spontaneous production (Ctrl).

Each dot represents a distinct donor. Horizontal continue lines depict the mean. Red dotted line depict control. Statistical differences were assessed by paired t-test. * = ≤ 0.05 .

189x276mm (300 x 300 DPI)

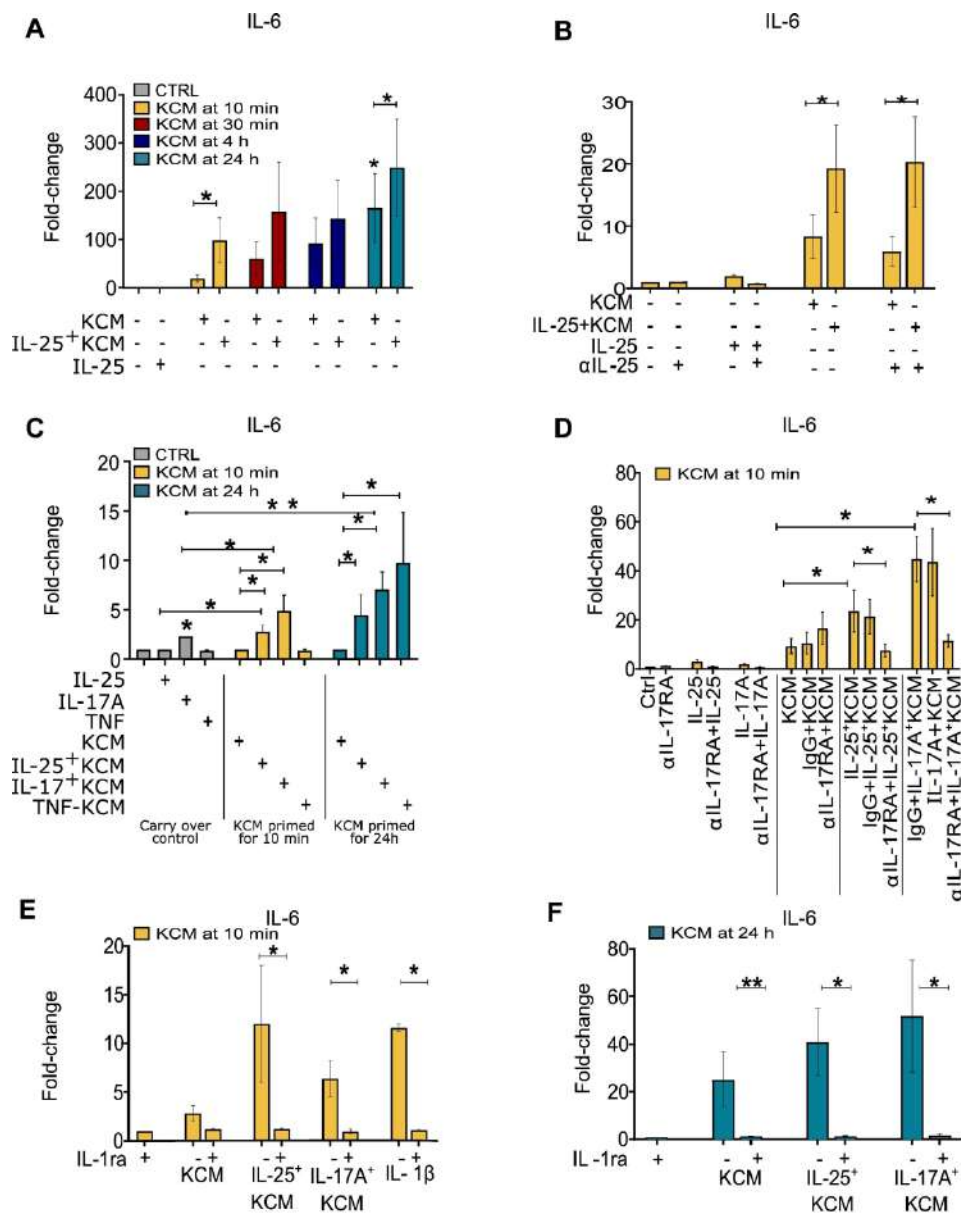


Figure 5

IL-25 promotes the release of fibroblast-activating factors by keratinocytes at early time points.

a) IL-6 production by HDF cultured with 12.5% control keratinocytes conditioned medium (KCM) or IL-25+KCM harvested at the indicated time points. b, d) anti-IL-25 polyclonal-Ab, anti-IL-17RA mAb, and irrelevant Ab (IgG) added to KCM (b) or keratinocytes (d) prior to HDF stimulation. c) HDF cultured with KCM, IL-25+KCM, IL-17A (IL-17A+KCM), or TNF (TNF+KCM) harvested after 10 min. e, f) IL-1ra (100 ng/ml) added to HDF before priming with KCM or IL-25+KCM collected at 10 min (e) or 24h (f). Results are expressed as fold-change from spontaneous production (Ctrl). For all panels $n \geq 3$; bars represent the mean \pm SEM. Wilcoxon signed-rank test was used to assess statistical significance. * $p \leq 0.05$; ** $p \leq 0.01$.

200x252mm (300 x 300 DPI)

IL-25 participates to keratinocyte-driven dermal matrix turnover and is reduced in Systemic Sclerosis epidermis

Barbara Russo, Julia Borowczyk, Pietro Cacialli, Philippe Moguelet, Marie-Elise Truchetet, Ali Modarressi, Nicolò C. Brembilla, Wolf-Henning Boehncke, Carlo Chizzolini

Supplementary material, methods, tables, figures

Supplementary Data S1

Cell cultures

Primary human dermal fibroblasts and keratinocytes were isolated from HD and SSc skin, as previously described (Dufour et al., 2020). Passage 2–3 keratinocytes were cultured in keratinocytes serum-free medium (KSFM, Gibco™, Paisley, United Kingdom), supplemented with rh-EGF and bovine pituitary extract. Seventy thousand cells/well were seeded in 6-well plates for 48 h, then starved for 6 h in KSFM without supplements and stimulated with IL-25 (100 ng/ml) or IL-17A (100 ng/mL) or TNF (1 ng/ml) (R&D Systems, Abingdon, United Kingdom), without supplements.

HD and SSc fibroblasts were used at passage 6–7 and cultured in triplicates in DMEM (Gibco, Paisley, United Kingdom), containing 10% fetal bovine serum (FBS) (Biowest, Nuaille, France), 1% non-essential amino acids, 1% L-glutamine, 1% sodium pyruvate, 50 U/ml penicillin, and 50 µg/ml streptomycin (all from Sigma, St. Louis, MO). Twenty thousand cells/well were seeded in 96-well plates for 24 h, then starved for 16 h in the absence of FBS, followed by stimulation with 12.5% of conditioned media (CM) from keratinocyte (K) primed or not with IL-25 (100 ng/ml), IL-17A (100 ng/ml), TNF (1 ng/ml) in DMEM containing 1% FBS, 25 µg/ml L-ascorbic acid, 3.4 µg/ml α-ketoglutaric acid, and 50 µg/ml β-amino propionitrile to favor collagen maturation, as well as 50 U/ml penicillin and 50 µg/ml streptomycin for 48 h before supernatant harvesting. KCM was added to fibroblasts in triplicates. For inhibition experiments, 8 µg/ml of anti-17RA monoclonal antibody (mAb) or 2.5 µg/ml IL-25 neutralizing antibody (Ab), or irrelevant Ab (R&D Systems), IL-1RA (100 ng/ml) (Kineret, Amgen, CA) was added to keratinocytes 30 minutes before stimulation with IL.17A (100 ng/mL) or IL-25 (100 ng/mL).

RNA sequencing analysis

RNA isolation from EE was performed with Qiagen RNAeasy microkit (Germany). Integrity and quantity of RNA were assessed with Bioanalyzer (Agilent Technologies, Santa Clara, CA) (RIN

1 ranging from 7.5 to 10). cDNA libraries were constructed using the Illumina TruSeq RNA
2 stranded Kit according to the manufacturer's protocol starting from poly-A RNA. Pools of 18
3 libraries were loaded at 2 nM for clustering on two lanes of a Single-read Illumina Flow cell.
4 Reads of 50 bases were generated using the TruSeq SBS chemistry on an Illumina HiSeq 4000
5 sequencer. FastQ reads were mapped to the ENSEMBL reference genome (GRCh38.89) using
6 STAR, version v.2.5.3a, with standard settings. The transcriptome metrics were evaluated
7 with the Picard tools v.1.141. The table of counts with the number of reads mapping to each
8 gene feature of the UCSC human hg38 reference was prepared with HTSeq v0.9.1. The
9 differential expression analysis was performed using R/Bioconductor package edgeR v.
10 3.18.1. Briefly, the counts were normalized according to the library size and filtered. The
11 genes were filtered on expression levels. As required by the experimental design paired t-test
12 was used to assess the differentially expressed genes. The differentially expressed genes p-
13 values were corrected for multiple testing errors with a 5% FDR (false discovery rate)
14 according to the correction by Benjamini-Hochberg (BH). The library preparation, sequencing,
15 and read mapping to the reference genome were performed by the Genomics Platform at the
16 University of Geneva (Switzerland).

17 In order to identify variation patterns related to biological and technical factors, we
18 performed Principal Component Analysis (PCA) by XLSTAT v2021.4 (by Addinsoft).

19 Heat Map with hierarchical clustering of expressed genes was executed using XLSTAT v2021.4
20 (by Addinsoft) .

21 The **D**atabase for **A**nnotation, **V**isualization and **I**ntegrated **D**iscovery (**DAVID**) v6.8 was used
22 for functional analysis differential expressed genes (DEG), using an EASE Score < 0.01 and a
23 max count of genes >3. Gene Ontology (GO) database was queried and only the DEG with FDR
24 < 0.05 a log fold change (logFC) \leq or \geq 2 were analyzed. We then performed cluster analysis
25 for the redundant annotation terms, using the Functional Annotation Clustering methods,
26 selecting high classification stringency. Subsequently pathway and network analysis were
27 performed using MetaCore™ (Cortellis Solution software; Clarivate Analytics, London, United
28 Kingdom). An FDR < 0.05 was used as a criterion to calculate if statistically significant DEGs
29 constituted a processor pathway.

Further enrichment analyses for DEGs were carried out with gGOST (g:profiler, by ELIXIR) (Raudvere et al., 2019) that brings together enrichments from several databases, those of our interest were the annotations from Gene Ontology (GO), Reactome and KEGG.

Datasets related to this article can be found at <https://www.ncbi.nlm.nih.gov/geo/query/acc.cgi?acc=GSE168312> under the accession number GSE168312.

Immunohistochemistry (IHC)

Skin biopsies were fixed in formaldehyde and embedded in paraffin. Five μ m slides were cut, deparaffinized in ultraclear and rehydrated in gradient concentrations of ethanol and water. Heat-induced antigen retrieval was performed in sodium citrate buffer pH6. Unspecific binding was blocked with horse serum, Vectastain kit (Vectorlab; Peterborough, United Kingdom). Slides were incubated with anti-IL-17E mAb (R&D Systems, Minneapolis, MN), as previously described (Borowczyk et al., 2020). Subsequently, incubations with secondary biotinylated universal antibody and streptavidin/peroxidase complex (Vectastain kit) were performed according to manufacturer instructions. Immunoreactivity was detected with ImmPACT AMEC Red from Vectorlab. Sections were counterstained with hematoxylin from Merck (Darmstadt, Germany). Full section images were acquired using Axioscan Z1 microscope (Carl Zeiss Microscopy GmbH) at 20X

Immunofluorescence (IF)

IL-25 immunofluorescence in SSc and HD skin was performed on formalin-fixed, paraffin-embedded sections (5 μ m). After paraffin removal, epitope retrieval with sodium citrate pH6, and blocking with 4% bovine serum albumin in phosphate-buffered saline, tissue sections were incubated with anti-IL-17E mAb (R&D Systems, Minneapolis, MN), as previously described (Senra et al., 2016). Subsequently, the AF488-conjugated secondary Ab was added. Nuclei were stained with DAPI Fluoromount-G (SouthernBiotech, Birmingham, AL). Laser-scanning confocal images were acquired using an LSM 800 confocal microscope and analyzed using ZEN software (Zeiss, Oberkochen, Germany). Sections incubated only with secondary Ab only were used as negative controls.

In situ hybridization (ISH)

The PCR template encompassing the coding region for the human IL-25 mRNA (exon 2 to 3) was generated from a plasmid containing the IL-25 full-length coding sequence (Myc-DDKtagged ORF clone of IL-25 in pCMV6 vector, Labforce). Template T-IL17E (7-461) was obtained by PCR using the forward hsa-IL25_SP6 (5'CCGATTAGGTGACACTATAGAACGCACACACACAAGCTAA 3') and reverse hsa-IL17E_T7 (5'CCGTAATACGACTCACTATAGGGGTTGCATTCTT GGCAATGGT 3') primers generating a PCR product of 455 bp length, as described (Senra et al., 2016). Digoxigenin-tagged antisense riboprobes were synthesized by *in vitro* transcription using the T7 RNA polymerase. ISH was carried out on formalin-fixed, paraffin-embedded tissue sections, as described (Cacialli et al., 2019), with some modifications. Briefly, sections were de-paraffined with ultraclear and progressively rehydrated. The sections were washed in PBS and postfixed for 20 minutes in PBS-PFA4%. The tissue was rinsed with PBS and treated 15 minutes with proteinase K (2 mg/mL) diluted in PBS at 37°C. The reaction was stopped in PBS before post-fixation and the slides rinsed three times in PBS. Sections were incubated overnight at 62.7°C with the probe (75 ng/slide) diluted in specific buffer (formamide 50%; SSC [saline sodium citrate] buffer 2X, Dehart 5X, yeast tRNA 50 µL/mL, EDTA 4 mM, dextran sulfate 2.5%). The slides were subsequently rinsed 30 minutes with SSC2X; SSC2x/formamide 50%, SSC 0.2x and SSC 0.1x. Then the slides were blocked with blocking buffer. Sections were incubated with an anti-digoxigenin antibody (1:2000) overnight. On the last day, slides were washed 2X for 10 min with PBT and then 3X with the staining solution containing Tris-HCl 100 mM (pH 9.5), NaCl (100 mM) and MgCl2 (10 mM). Finally, the slides were incubated 24h in staining solution with NBT/BCIP (50 mg/ml). After fixation with PFA4%, the slides were counterstained with Nuclear fast red. Sense probe was used as negative control. Full section images were acquired using Axioscan Z1 microscope (Carl Zeiss Microscopy GmbH) with 20X magnification.

Histological analysis

Images were analyzed by Matlab R2c18b (The MathWorks, Natick, Massachusetts, USA). A Matlab algorithm was developed by the bioimaging facility of the University of Geneva to quantify IHC/IF for IL-25. The software was designed to detect MFI (mean fluorescence intensity) or optical density (for IHC images) in every 2µm from basement membrane to the granular layer .

ELISA

Quantification of IL-6, IL-8, MMP-1, Collagen-I, and fibronectin levels by DuoSet ELISA kits was performed according to the manufacturer's instruction (R&D Systems, Abingdon, United Kingdom). For each culture condition, biological triplicates were tested by ELISA.

Quantitative PCR (qPCR)

mRNA was extracted by Zymo research quick RNA isolation kit (LucernaChem AG, Switzerland) according to the manufacturer recommendations. SYBR green reactions were performed in triplicate on a StepOne Plus (Applied Biosystems). Raw Ct values obtained with SDS 2.2.1. software (Applied Biosystems) were analyzed and two stable housekeeping genes (GAPDH and 18s RNA) were used for normalization. Oligonucleotides were obtained from Invitrogen (MMP1, COL1A1, COL1A2) and Microsynth (GAPDH, 18s RNA).

Western Blot

Fibroblasts were lysed for 10 minutes on ice in RIPA Buffer (Sigma-Aldrich, Darmstadt, Germany) supplemented with protease and phosphatase inhibitor cocktail (Merck, Schaffhausen, Switzerland). Protein extracts were centrifugated and stored at -20°C until used. For Western blotting, 12 µg of total protein extract was separated in 10% sodium dodecyl sulfate–polyacrylamide gel electrophoresis, under reducing conditions, and electro-blotted onto nitrocellulose membranes (Amersham Hybond enhanced chemiluminescence [ECL]; GE Healthcare Zurich). Blots were incubated with mouse anti- α SMA (Abcam) or anti-MMP9 (Abcam) or anti- α tubulin (Sigma) antibodies, followed by incubation with peroxidase-conjugated mouse antiserum. An ECL blotting analysis system (Thermo Fisher Scientific, Massachusetts, USA) was used for antigen–antibody detection. Quantification analysis was performed with ImageJ software (<http://rsbweb.nih.gov/ij>) and values were normalized to those for α -tubulin.

References

Borowczyk J, Buerger C, Tadjrischi N, Drukala J, Wolnicki M, Wnuk D, et al. IL-17E (IL-25) and IL-17A Differentially Affect the Functions of Human Keratinocytes. The Journal of investigative dermatology 2020;140(7):1379-89.e2.

Cacialli P, Gatta C, D'Angelo L, Leggieri A, Palladino A, de Girolamo P, et al. Nerve growth factor is expressed and stored in central neurons of adult zebrafish. J Anat 2019;235(1):167-79.

Dufour AM, Borowczyk-Michalowska J, Alvarez M, Truchetet ME, Modarressi A, Brembilla NC, et al. IL-17A dissociates inflammation from fibrogenesis in systemic sclerosis (scleroderma). J Invest Dermatol 2020;140(1):103-12.

Raudvere U, Kolberg L, Kuzmin I, Arak T, Adler P, Peterson H, et al. g:Profiler: a web server for functional enrichment analysis and conversions of gene lists (2019 update). Nucleic Acids Res 2019;47(W1):W191-w8.

Senra L, Stalder R, Alvarez Martinez D, Chizzolini C, Boehncke WH, Brembilla NC. Keratinocyte-Derived IL-17E Contributes to Inflammation in Psoriasis. The Journal of investigative dermatology 2016;136(10):1970-80.